Compressively Sensed Hybrid PET/MR Imaging with Enhanced Spatial Resolution

Krzysztof Malczewski

Poznan University of Technology
Polanka 3 60965 Poznan
Poland
kmal@et.put.poznan.pl

Abstract— **Considering the success of PET/CT modalities, public expectations for any new combination, such as MR/PET are pretty high. Since MRI does not utilize any ionizing radiation its use is recommended in preference to CT when either modality could yield the same information. Thus, it turns into a perfect anatomical complement to PET. The principal idea behind merging PET and MRI is to combine the functional / metabolic information provided by PET with the high soft-tissue contrast and the functional information offered by MRI. This article presents the new compression sensing based super-resolution algorithm for improving the image resolution in clinical MR-PET hybrid scanners. Despite MR and PET each provide unique and independent information they share the same underlying anatomical features. Hence, rather than treating the data from PET and MR singly, we are able to incorporate both data sets in a simultaneous reconstruction algorithm. A joint sparsity based reconstruction method for multiple sensors, allows these anatomical similarities to improve the two unique and independent data sets. It is shown that the presented approach improves MR-PET spatial resolution in cases when Compressed Sensing (CS) sequences are used. Compressed sensing (CS) aims at signal and images reconstructing from significantly fewer measurements than were traditionally thought necessary. The application of CS in medical modalities has the potential for significant scan time reductions, with visible benefits for patients and health care economics. These methods emphasize on maximizing image sparsity on known sparse transform domain and minimizing fidelity.**

Keywords—MRI, PET, compressed sensing, super-resolution

I. INTRODUCTION

The PET/MRI scanners have been available on market for a couple of years. It has been confirmed that they provide a clear benefit. It is shown that these devices are useful for particular applications demanding multiparametric imaging capabilities, high soft tissue contrast and/or lower radiation dose. However, the demand for a better resolution in all medical imaging applications still remains a serious research challenge. Most imaging applications highly depend on high-resolution imagery. Enhancing image resolution by improving detector array resolution is not always a possible solution to increasing resolution. It is evident that each imaging device has its own inherent resolution, which is determined based on the physical constraints of the system detectors that are in turn tuned to signal-to-noise and timing considerations. A common goal across SRR systems is to enhance image resolution, and as much as possible. SR technology has been proved to be useful in medical imaging modalities including Magnetic Resonance Imaging (MRI) [1], functional Magnetic Resonance Imaging (fMRI), Computed Tomography (CT) and Positron Emission Tomography (PET) [1]. PET/CT and other combined scanners have in the last years quickly emerged as important research tools and are proving to be invaluable for improved diagnostics in routine nuclear medicine. The design of hybrid PET/MR scanners revealed a serious technical challenge, and only recently were these instruments introduced to the market. Preliminary performance expectations have been high, notably because of the potential for superior MRI tissue contrast, as well as the potential for PET functional imaging. Positron emission tomography (PET) is a major in vivo biomedical imaging modality that provides spatial information on the biochemical, functional, and molecular processes taking place in the living body. PET has unique roles during the evaluation of many diseases and is a key research tool during studies on experimental animals [2].

In this paper, the author proposes a novel PET/MRI related technique, which combines super-resolution, motion correction procedures and compressed sampling. The results argued its compellingly in experimental studies. Comparison between the SR image and low-resolution images exhibits batter resolution and higher number of details. The presented SR algorithm may replace the present approach in current hybrid scanners without any hardware modifications. A key advantage of the method is that it doesn't neglect the motion correction issue. Moreover, it leads to higher spatial resolution keeping reasonable scanning times.

II. HYBRID MR-PET

In recent years, development of hybrid-imaging instrumentation has been indicated as one of the innovations with the strongest impact on diagnostic imaging in clinical routine. The main reason behind these developments is the significant extent to which several different imaging modalities reveal complementary rather than redundant features.

Therefore, it is reasonable to employ the particular strengths of different modalities, and to compensate particular disadvantages of one modality with capabilities of another by combination of the different modalities into one "hybrid"

device. First hybrid PET/CT scanners have been introduced to the market in around 2000 [3] and gained their importance, thereby quickly obviating the demand for PET-only scanners. This accomplishment has been strongly motivated by oncological applications, combining the high sensitivity of PET with the anatomical accurateness of CT.

The fusing of 18F-FDG, a tracer for metabolic activity with CT, has especially proved highly valuable [4]. The FDG-PET leads to the sensitive detection of tumor cells and the estimation of their viability (e.g. for therapy control). The CT [5] shows the exact anatomic localization of suspect lesions and has a very high sensitivity for small lesions that are missed by PET because of the limited resolution or movement artifacts (e.g. caused by respiratory motion). However, CT has some particular restrictions, the most apparent being the relatively low soft-tissue contrast. This characterizes a disadvantage principally for diagnostic issues directed to body regions that are defined by a complicated regional arrangement of different adjacent soft tissue structures. This scenario may happen to the brain region as well as to the head-and-neck area or the pelvis. In turn, MR-imaging is popular for the ability to deliver excellent soft-tissue contrast. This is the key argument why corresponding diagnostic problems are typically addressed to MRI as the first-line imaging procedure of choice rather than to CT. This involves questions concerning e.g. neurological disorders, brain tumors, conditions in the head and neck region, abdominal/hepatic and pelvic masses and musculoskeletal disorders. PET has proved its value as a complementary test in itself, while frequently being conducted in addition to required MRI-routines.

Hence, the usefulness of a combining of PET with MRI seems undisputed [6]. Though, the development of this hybrid MR/PET scanner has been postponed for a long time primarily by technical obstacles which have been harder to overcome compared to the combination of PET and CT. While these techniques represent modalities dealing with radiation (although in different wavelengths) and can thus be merged more easily. PET and MRI have different image acquisition principles. The strong magnetic field needed for successful MR-image acquisition is severely affecting the acquisition of the PET-signal. Especially, the regular photomultiplier method widely used for obtaining the PET signal does not work properly in a magnetic field. To avoid this limitation, modalities have been developed in which spatially separate MR- and PET-scanners are connected by means of a moving table. The patient is located on this table and experiences first PET and then MR imaging, without having to get up from the table between the scans. Nevertheless, this model does not allow simultaneous image acquisition and this is of course associated with lengthy examination protocols and with the risk of patient movement.

While Positron Emission Tomography (PET) has great functional and quantitative capabilities, it does not provide by itself high-resolution images. This limitation could be overcome by integrating PET with other imaging modalities such as CT or MRI.

III. MR-PET JOINT SPARSITY

The expansion of MR-PET scanners allowed for simultaneous acquisitions of PET and MR data [7]. Though, the images are being reconstructed separately and often projected onto each other. True joint-reconstruction of both MR-PET could improve the resolution and image quality of both data sets. While MR and PET each provide unique and independent information, they share the same underlying anatomical features. This feature may be used in combination with other extracted structures to minimize motion artifacts. Hence, rather than considering the data from PET and MR separately, we can associate the two data sets in a synchronized reconstruction process. A combined sparsity based reconstruction method for multiple sensors supporting the super-resolution allows these anatomical similarities to enhance the image resolution, remove the motion artifacts and improve the two unique and independent data sets.

The suggested method reconstructs multi-dimensional data by treating the two imaging modalities as additional dimensions of a single dataset, solving the following optimization problem:
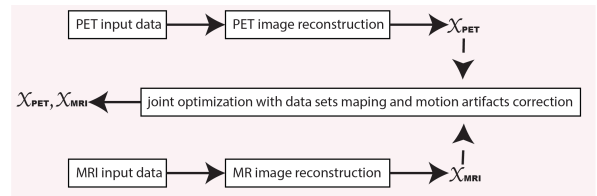
Figure 1 . The algorithm incorporates the two modalities joint sparsity. The super-resolution algorithm has been neglected for its simplicity.

In this equation xMR and xPET promote their data sets sparsity by using the Compressed Sensing framework. Moreover, they represent the 3D image data sets corresponding to the MR k-space and PET sinogram. The algorithm considers multiplication by coil sensitivities, maps data between MR images and k space. The joint sparsity issue is the most important subject of cooperating of anatomical information between PET and MR datasets, and it could be expressed as follows:

$$\left\| \begin{array}{c} \Psi\left(x_{MRI}^{i}\right) \\ \Psi\left(x_{PET}^{i}\right) \end{array} \right\|_{2} = \sqrt{\left(\Psi\left(x_{MRI}^{i}\right)\right)^{2} + \left(\Psi\left(x_{PET}^{i}\right)\right)^{2}}$$

Moreover, "an individual" sparsity term is associated with the MR dataset in order to remove undersampling artifacts and decrease the acquisition time.

The numerous authors [7] recognized a spatially dependent regularization considered as the difference of the signal intensities in each voxel i :

$$d^{i} = \left\| \psi\left(x_{MR}^{i}\right) \right\| - \left\| \psi\left(x_{PET}^{i}\right) \right\|$$

The regularization parameters ensure that joint information is shared only between the two modalities in areas where the

projected data sets are coherent, see figure above. The algorithm presented in this paper utilizes "double" sparsity, i.e. in MRI and PET domains. For these reasons, the author gives a sense of both aspects.

IV. MRI DATA ACQUISITION ISSUES

Some previous studies have struggled with acceleration issues. In this way, numerous sampling patterns such as spiral, radial, balanced steady-state free precession [1], view sharing [8], PROPELLER and other parallel imaging approaches have been tested. Among these acceleration methods, the most widely used method for MRI is parallel imaging [9]. Most MR devices loaded with coil arrays are able to modify sampling scheme including PROPELLER, generalized autocalibrating partially parallel acquisitions (GRAPPA) [10] or sensitivity encoding (SENSE) [11]. It usually leads to acceleration rates of 2–3. In turn, Compressed sensing (CS) procedures, relatively recently introduced may lead to further acceleration of MRI procedures. MRI seems to be a perfect candidate for applying CS, because of its steady state of magnetization. Moreover, the temporal variation in signal is limited to blood vessel regions, and the resulting image data are sparse after applying an appropriate orthogonal transform. The authors in [11-15] have proposed temporal principal component analysis (PCA) as the sparsifying transform. However, scan time reduction in magnetic resonance imaging (MRI) remains an important issue, especially when considering acquisition of medical images in a clinical setting. Shortening of acquisition times offers reduction of costs and it also increases a patient throughput and comfort. Recently presented a combination of compressed sensing and parallel imaging, i.e. k-t SPARSE-SENSE [16,17] argued compellingly for using this technique for accelerating perfusion studies. Unfortunately, this approach is highly sensitive to various type of motion, such as respiration related movement which decreases its temporal sparsity and implies temporal blurring in the reconstructed images. The sparsity in Magnetic Resonance Imaging (MRI) is applied to significantly undersample k-space. Compressed sensing MRI may become an essential medical imaging tool with an inherently slow data acquisition process. Combining CS and MRI offers potentially significant scan time reductions, with benefits for patients and health care economical factors [18]. Technically, MRI requests two major aspects for successful application of CS [19]: a. medical imagery is physically compressible by sparse coding in an appropriate transform domain (e.g., by wavelet transform), and b. MRI scanners are able to acquire encoded samples. The compressed sensing theory is available even from the samples harvested at lower than the Nyquist rate as long as the unknown image is sparse or compressible.

V. COMPRESSED SENSING IN MRI

Planning a CS scheme for MRI it can now be expressed as selecting a subset of the frequency domain. It can be efficiently sampled and is incoherent with respect to the sparsifying transform. Before the notion of incoherence will be introduced we should note that narrow optimization of incoherence must not be pushed too far [19]. Some of the most impressive and powerful results about CS assume one samples a completely random subset of k-space, which indeed gives

very low coherence [20]. Though random sampling is an inspiring and instructive idea, sampling a truly random subset of k-space is generally impractical. All the practical sampling trajectories must satisfy hardware and physiological constraints. Hence sampling trajectories must follow smooth lines and curves. Furthermore, a uniform random distribution of samples in spatial frequency does not take into account the energy distribution of MR images in k-space, which is far from uniform. Most energy in MRI is concentrated close to the center of k-space and rapidly decays towards outside of k-space. Therefore, eligible patterns for CS in MRI should have variable density sampling with denser sampling near the center of k-space, matching the energy distribution in k-space.

Latest advances in compressed sensing theory reveals that sensing matrices whose elements are drawn independently from certain probability distributions guarantee exact recovery of a sparse signal from "an incomplete" number of measurements with high probability. Due to practical reasons it cannot be formulated in this way. In turn it could take Toeplitz matrix form. This fact prompted the authors [20] to consider Toeplitz block matrices as the sensing matrices. Technically all the sampling scheme parts are compressed and they are sparse. Formally, semi-PROPELLER k-spaces have been acquiring by compressive-sensing native PROPELLER blades., see figure below.
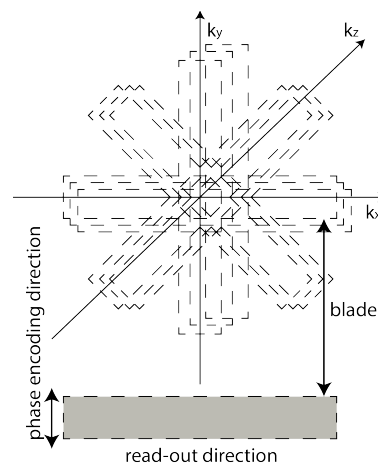
Figure 2. Semi-PROPELLER sampling pattern.

A formal approach for reconstruction could be briefly described in the following way. Let's represent the reconstructed image by a complex vector *m*. The ψ denotes the linear operator that transforms from pixel representation into the chosen representation. Let F_s denote the undersampled Fourier transform, corresponding to one of the k-space undersampling schemes. The reconstructions are obtained by solving the following constrained optimization problem:

$$\text{minimize } \|\psi m\|_1$$

$$\text{s.t. } \|F_s m - y\|_2 < \varepsilon$$

where *y* is the measured k-space data from the MRI scanner and ε controls the fidelity of the reconstruction to the

measured data. The threshold parameter ε is roughly the expected noise level. The l_1 norm means $\|x\|_1 = \sum_i |x_i|$.

Minimizing the l_1 norm of $\|\psi m\|_1$ promotes sparsity [19]. The constraint $\|F_s m - y\|_2 < \varepsilon$ enforces data consistency. Formally, among all the solutions that are consistent with the acquired data, we want to find a solution that is compressible by the transform ψ. It is worth mentioning that when finite-differencing is used as the sparsifying transform, the objective becomes the well-known total variation (TV) penalty [19].

In this paper the author tested the application of CS to brain imaging by acquiring a full Nyquist-sampled data set which has been retrospectively undersampled. For each slice a different random subset of 80 trajectories from 192 possible trajectories has been tested. It implied a speedup factor 2.4. It has been shown that undersampling each slice differently reduces coherence compared to sampling the same way in all slices [6].

VI. INTER MRI-PET SIMULTANEOUS REGISTRATION ALGORITHM

Precisely, image registration represents a highly non-convex optimization due to the coupling conditions that must be satisfied. Typically this problem is highly ill conditioned and tends to local minima. Recently some researchers have argued that this kind of disadvantages could be overcome using discrete optimization algorithms. In this paper the author employs the new method called "deeds" utilizing a discrete dense displacement sampling for the deformable registration of high-resolution [21] volumes. In this method the image is characterized as minimum spanning tree.
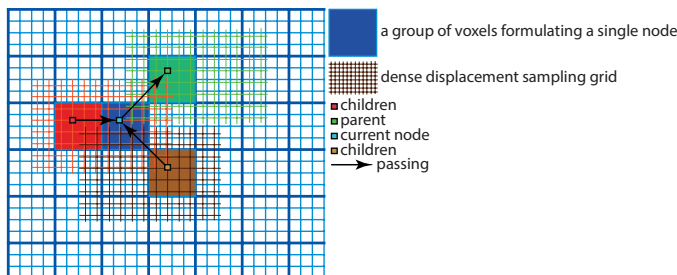
Figure 3. An example of minimum spanning tree (MST)

These kinds of constraints formulate cost functions that are being globally optimized via dynamic programming. It enforces the smoothness of the deformations. The usage of this method provides to significantly lower registration errors than for other state-of-the-art registration techniques, especially in the presence of big deformations.

Discrete optimization is usually performed as Markov Random Field (MRF labelling. For the purposes of our non-parametric image registration framework, a graph is defined, in which the nodes $p \in P$ correspond to voxels (or group of voxels) and in which, for each node, there is a set of (hidden) labels f_p, which correspond to discrete

displacements. The energy function to be optimized consists of two terms: the data (also called unary) cost D (which is independent for each node); and the pair-wise regularization cost $R(f_p, f_q)$ for any node q, which is directly connected $(\in N)$ with p:

$$E(f) = \sum_{p \in P} D(f_p) + \alpha \sum_{(p,q) \in P} R(f_p, f_q)$$

The cost function presented above measures tracks two images voxel similarity. Technically, this factor is independent of the displacements of its neighbors.

The α is a weighting parameter which specifies the influence of the regularization.

In the method adopted above the global optimum is found for a complex 3D registration problem with a very large (dense) label space within minutes using a reduced neighborhood interaction based on a minimum spanning tree (MST). The MST refers to a spanning tree with minimum total edge costs. This method reflects the underlying anatomical connectivity in a MRI image (see figure above).

It is clearly seen that the maximum width is approximately $|P| / \log|P|$. The Prim's algorithm product is a sorted list of all the nodes and the index of each node's parent respectively.

The global optimum is being found in the following way.

At each node p, the cost C_p of the most appropriate displacement could be calculated, given the displacement f_q of its parent q:

$$C_p(f_p) = \min_{f_p} \left(D(f_p) + R(f_p, f_q) + \sum_c C_c(f_p) \right)$$

where c are the p offspring.

The most relevant displacement could be found by replacing min with argmin in the equation 2.

For all the leaf nodes the above equation could be calculated directly. Afterward, the tree is expressed from its leaves down to the root node.

To avoid local minimum issues, the authors [deeds] suggested a multi-level scheme, in which they only employ the highest resolution image. For a given level, the image is subdivided into non-overlapping cubic groups of voxels. The similarity cost is first calculated for each voxel separately using dense displacement sampling, and then aggregated for all voxels of the same group (this forms an additional intrinsic regularization and reduces the number of nodes). Subsequently, the regularization term is calculated only for each group of voxels (see MST figure). Using this approach, both high spatial accuracy and low computational complexity are achieved.

VII. MRI CS AND SR BLENDING

Combining the IBP algorithm and the estimated motion parameters, the super-resolution image is iteratively reconstructed. Starting with an initial guess f_0 [22] for the high resolution image, the imaging process is simulated to obtain a set of low resolution images $\{g_k^{(0)}\}$ corresponding to the observed input images $\{g_k\}$ If f_0 were the correct high resolution image (1), then the simulated images $\{g_k\}$ should be identical to the observed images.

The difference images $(g_k - g_k^n)$ are used to improve the initial guess by "back projecting" each value in difference images onto its coresponding field in f_0, yielding an improved high-resolution image f_1. This process is repeated iteratively to minimize the remaining error. This iterative update scheme can be expressed by:

$$f^{(n+1)} = f^{(n)} + \frac{1}{K}\sum_{k=1}^{K} T_k^{-1}\left(\left(\left(g_k - g_k^{(n)}\right)\uparrow s\right) * p\right)$$

(2)

Where K is the number of low-resolution images $\uparrow$ arrow an upsampling operator by a factor s and p is a back projection kernel determined by h and T_k. Taking the average of all discrepancies has the effect of reducing noise.
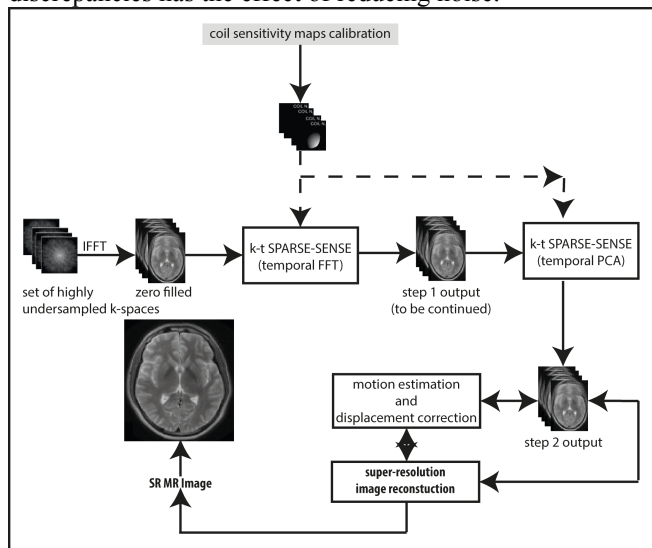
Figure 4 1 The proposed algorithm chart flow

VIII. COMPRESSIVELY SENSED PET SIGNALS

The common goal of the main algorithm is to compressively sense all the input signals as much as possible. In this chapter author claims that PET signals compressed sensing is feasible.

Radioactive substances that emit positrons are frequently being multiplexed to reduce the number of readout channels.

These multiple signals could be combined into super-resolution PET image. This framework part aims at combining the super-resolution and compressed-sensing in MR-PET hybrid systems. Fortunately, the underlying detector signals have a sparse representation. Thanks to this feature sparse-sense may be applied for developing new multiplexing schemes. One of CS key aspect is formulating relevant sensing matrices. Random methods may be applied to create them in the way that they satisfy the restricted isometry property.

The method of formulating sensing matrices is a maximum likelihood framework. It allows for developing a new method for constructing multiplexing (sensing) matrices that will be able to recover signals more accurately in a mean square error sense compared than any other sensing matrices constructed by random construction methods [22].

The main features of the algorithm methodology adopted over here are spatial multiplexing methods that have the ability to resolve the position and energies of interactions that occur in multiple crystal elements with the constant time sampling interval. The detector signals are being discretized in both the spatial and time domain.

Technically, a mathematical model describing readout spatial multiplexing for this type of PET detector can be expressed by an undetermined linear system of equations mapping the crystal elements to a set of readout channels at one time point.

The detector readout can be characterized by following formula:

$$y = C(x + nx) + e$$

Where the matrix C defines the multiplexing network that maps the d detector pixels into the m readout channels where $d > m$ and e is an additional random measurement noise vector produced by the multiplexing electronics.

Each readout is represented by a linearly weighted sum of the photodetector pixels with weights described by the matrix C.

A p-subdictionary is a matrix formed by using p codes of the dictionary.

This system model is commonly applied in medical imaging applications besides PET such as SPECT and X-ray CT.

The further goal is to recover the original position and magnitudes of detected events on the image array x by decoding the multiplexed readouts y at each time point or sampling interval.

Formally, mathematical model for describing spatial multiplexing readouts is expressed as a sparse signal recovery framework.

The compressed sensing methods such as L0 -norm and L1-norm minimization of random sensing matrices are not sufficiently noise robust for PET is the certainly, not without significance. This is the reason why a new method for improving the L0 -norm minimization decoder and for constructing sensing matrices with better SNR for PET detectors compared to other compressed sensing, Anger

multiplexing, and cross-strip multiplexing have been developed.

Moreover, a nonlinear reconstruction must be done to impose both sparsity of the image representation and consistency with the acquired data. Compressed sensing may be used to multiplex a large number of individual readout sensors to drastically reduce the number of readout channels in a large area PET block detector. The compressed sensing idea can be utilized to treat PET data acquisition as a sparse readout problem and achieve sub-Nyquist rate sampling, where the Nyquist rate is determined by the pixel pitch of the all individual SiPM sensors. In this way, the sensing matrix is prepared by using discrete elements or wires that uniquely connect pixels to readout channels [22]. Technically, by analyzing the recorded magnitude on several ADC channels, the original pixel values can be recovered even though they have been scrambled through a sensing matrix. In a PET block detector design comprising 128 SiPM pixels arranged in a 16 × 8 array, compressed sensing can provide higher multiplexing ratios (128:16) than Anger logic (128:32) or Cross-strip readout (128:24) patterns while resolving multiple simultaneous hits. Unlike Anger and cross-strip multiplexing, compressed sensing may recover the positions and magnitudes of simultaneous, multiple pixel hits. Interpreting multiple pixel hits can be applied to improve the positioning of events in light-sharing designs, inter-crystal scatter events, or events that pile up in the detector.

IX. SUPER-RESOLUTION IN PET AND ITS REGULARIZATION ALGORITHM

Basing on MR-PET joint sparsity and its common product features, the MR data sets based motion model parameters we can utilize them to promote the PET image enhancement. Formally, the same super-resolution algorithm is exploited, see figure below.
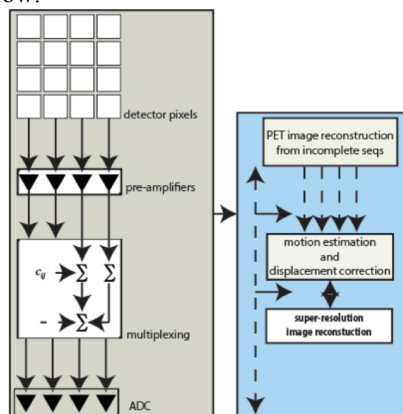
Figure 5. The PET input sensing.

X. DISCUSSION AND EXPERIMENT

In this paper, the practicability of implementing super resolution into PET scans has been exposed.

The method has been applied using Biograph mMR scanner data sets and internal organ shifts as well as transaxial rotational displacement. In this way two different sets were acquired. The first one with all detectors operational (baseline) and once with 8 equidistant detector blocks turned off (partially sampled, 12% detectors have been turned off. The resulting partially sampled sinogram is after that split into two different components, each sparsely represented in a specific transform domain.

An iterative numerical optimization algorithm was then used to recover the PS sinogram based on the solution of a combination of conjugate gradient, underdetermined system of equations and block-coordinated relaxations. In addition, the total variation has been minimized for the first component to direct it into much more convenient a piece-wise smooth model. Finally the two components were added together to achieve the sinogram, which was used to compare with the original PS sinogram. Compressed sensing seems to be the perfect choice for recovering PS PET data. This approach can potentially be used to generate PET images with accurate quantitation while reducing number of detectors/ring.

XI. CONCLUSION AND KEY BENEFITS

PET/CT and other combined scanners have gained their importance over the last decade. Understanding the nature and purpose of these tools is thus the first step to becoming an important subject of research area. The proposed algorithm may reduce artifacts caused by undersampled data, even in the presence of motion.

This report presents the successful use of a super-resolution algorithm to enhance the resolution of MR/PET images. With an increase in scan time for one FOV, a patient trial showed that the super-resolution technique in the axial direction is feasible in a clinical setting without increasing the radiation dose and with no changes in hardware. As expected, the proposed method improves the spatial resolution, but also enhances noise and artefacts. This effect becomes more visible as the number of super resolution image reconstruction algorithm iterations increases. Preliminary trial results show that the super-resolution approach can be applied to MR/PET imaging, noticeably improving the spatial resolution achievable. During an emission tomography study, induced motion due to patient breathing can lead to artifacts in the reconstructed image. This factor may produce less accurate diagnosis and more important, incorrect radiotherapy planning. The methodology to correct for respiratory motion in the super-resolution image reconstruction step has been developed. It resulted in motion artifacts free scan. The results without a doubt demonstrate an improvement in resolution and contrast ratio, see figure 3.

The increase in anatomical detail in the functional PET image aids in the registration of the image with a corresponding anatomical image from another modality such as MRI. This would especially be of significance in scanners, which are dual-modality. The super-resolution technique presented here provides a method of approaching these resolution goals with available clinical MR/PET scanners.

Higher resolution of PET images may have several implications in research and clinical practice. However, all the

studies are limited by the spatial resolution of the presently available instrumentation. Higher PET resolution would be especially helpful for improving sensitivity for detection of small tumors. Higher resolution PET images provided by a super-resolution algorithm may show a more differentiated anatomical structure, see Figure 3. The design of hybrid PET/MR is still an open issue and has been recognized as the grand challenge of the next years. Results presented above are preliminary and subject to completion. The expectations related to their performance are high, mostly because of the potential for superior tissue contrast inherent in the MR modality, as well as the potential for multiparametric functional imaging in conjunction with PET. This work struggles with combining PET/MR with compressed sensing and super-resolution. This modality faces the financial aspects and this issue needs to be considered. Therefore, whether the higher acquisition costs for PET/MR will be balanced in the long-term still needs to be confirmed.
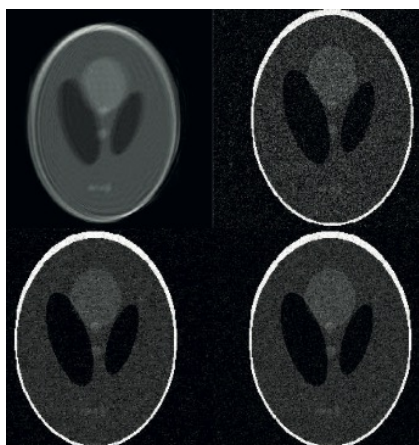
Figure 6. From the upper left to the lower right: the uncorrected image after motion consisting of a modeled shift occurring over the course of the entire acquisition time and reconstruction result and the reconstruction results of the Shepp-Logan phantom. The sampling rates are 25, 40, and 60 percent from left to right, respectively.
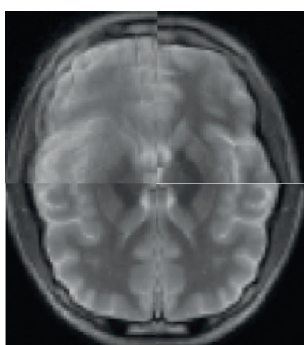
Figure 7. The 4 quarters. From left to right. Upper row: downsampled and no motion correction applied, downsampled and motion correction applied. Lower row: motion corrected regular sampling scheme (with no downsampling applied), super-resolution CS with motion compensation (proposed algorithm).

The experiment has been conducted for two different types of input data. All the initial experiments were conducted on a 1.5T MR Signa Excite scanner sequences. All the CS reconstructions have been implemented in Matlab. Furthermore, two different linear schemes were applied for comparison; zero-filling with density compensation (ZF-w/dc) and reconstruction from a Nyquist sampled low-resolution (LR) acquisition. The LR acquisition has been obtained from centric-ordered data with the same number of data samples as other undersampled sets, see figure 2. The goal of simulation was to examine performance of the compressively sensed super-resolution image reconstruction compared to the LR and Zero Filling with density compensation methods. The further objective was to present superiority of variable density random undersampling over uniform one. Hence, sets of randomly undersampled data with uniform density as well as that with variable density have been constructed from "full" irregularly sampled k-space trajectories. In this test a T2-weighted multislice k-space data of a brain has been analyzed. Figure 2 shows simulation results. While each CS exhibits a decrease in SNR because of the incoherent interference, the uniform density undersampling interference is much more visible and more "structured" than that for variable density. It is worth underlining that CS leads to acquisition acceleration when compared to the regular k-space sampling pattern. This framework part aims at combining the super-resolution and compressed-sensing in MRI scanners.

The second subsection goal is to illustrate inverse problems of compressed sensing for MRI on phantom data. In particular, the author shows reconstruction examples of the Shepp-Logan phantom from sparse projections, with 25 and 12 radial lines in FFT-domain as welll as reconstruction from limited-angle projections, with a reduced subset of 60 projections within a 90 degrees aperture. Technically semi-PROPELLER k-spaces have been acquiring by compressive-sensing native PROPELLER blades. The low-resolution acquisition has been included in centric-ordered data with the same number of data samples as the undersampled sets, see figures 3 and 5.

Figure 8. The Shepp-Logan phantom results comparison. From the left: the PROPELLER sampling matrix reconstruction output, the proposed algorithm result with enhanced resolution. The lower row exposes detailed images.
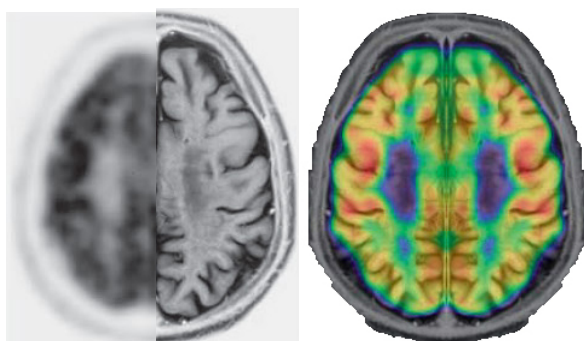
Figure 9. A patient case. From left to right: The axial slices reveal the PET (A) and MR (B). The images have been captured at each position of the resected brain strcutures. and the resulting MR/PET data set (the last two quarters) - no signs of motion artifacts.
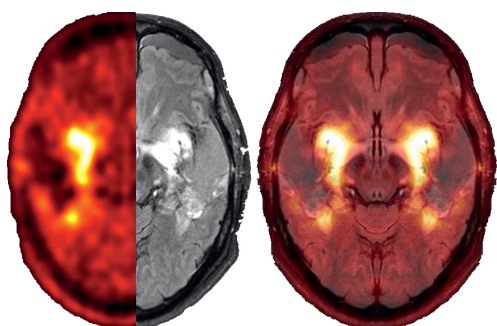
Figure 10. A: An example of 18F-FET PET scan. B: MR-image, the last two quarters represent: Fusion of PET and MR data sets.
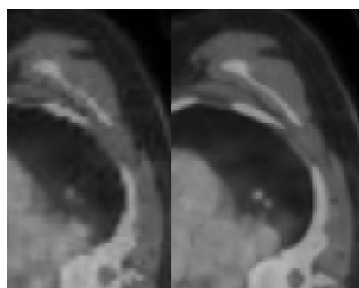
Figure 11. Giant Cell Arteritis Axial fused PET/CT image showing diffuse abnormal FDG uptake in the brachiocephalic and subclavan arteries. From left to right: conventional PET with CS, the super-resolution image with motion correction.
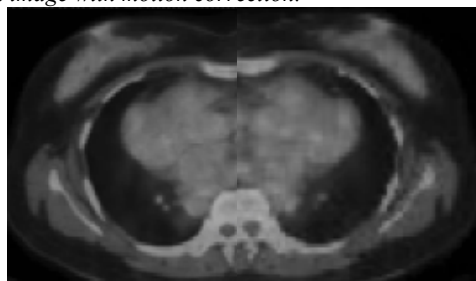
Figure 12. Giant Cell Arteritis Axial fused PET/CT image showing diffuse abnormal FDG uptake in the brachiocephalic and subclavan arteries. From left to right: conventional PET with CS, the super-resolution image with motion correction.

REFERENCES

K. Malczewski, „ Breaking The Resolution Limit In Medical Imaging Modalities", The 2012 International Conference on Image Processing, Computer Vision, and Pattern Recognition (IPCV'12), Worldcomp 2012, Las Vegas USA.

Fueger BJ, Czernin J, Hildebrandt I, Tran C, Halpern BS, Stout D, Phelps ME, Webe WA. 2006. Impact of animal handling on the results of 18F-FDG PET studies in mice. J Nucl Med 47:999–1006.

Beyer T, Townsend DW, Brun T, et al. A combined PET/CT scanner for clinical oncology. J Nucl Med 2000;41:1369–1379

Som P, Atkins HL, Bandoypadhyay D, Fowler JS, MacGregor RR, Matsui K, Oster ZH, Sacker DF, Shiue CY, Turner H, Wan CN, Wolf AP, Zabinski SV (1980). "A fluorinated glucose analog, 2-fluoro-2-deoxy-D-glucose (F-18): Nontoxic tracer for rapid tumor detection". J Nucl Med 21 (7): 670–675

Herman, G. T., Fundamentals of computerized tomography: Image reconstruction from projection, 2nd edition, Springer, 2009

Antoch, Gerald; Bockisch, Andreas (2008). "Combined PET/MRI: a new dimension in whole-body oncology imaging?". European Journal of Nuclear Medicine and Molecular Imaging 36 (S1): 113–120

F. Knol, et all." Joint reconstruction of simultaneously acquired MR-PET data with multi sensor compressed sensing based on a joint sparsity constraint", 3rd Conference in PET/MR and SPECT/MR Kos Island, Greece. 19-21 May 2014

Markl M, Hennig J.: Phase Contrast MRI with High Temporal resolution by view sharing. P Intl Soc Mag Reson Med, 2001

Griswold MA, Jakob PM, Heidemann RM, Nittka M, Jellus V, Wang J, Kiefer B, Haase A. (2002). Generalized autocalibrating partially parallel acquisitions (GRAPPA). Magn Reson Med. 47(6):1202-1210.

Pruessmann KP, Weiger M, Scheidegger MB, Boesiger P (1999). SENSE: sensitivity encoding for fast MRI. Magn Reson Med. 42(5):952-62

Jung H, Sung K, Nayak KS, Kim EY, Ye JC. k-t FOCUSS: a general compressed sensing framework for high resolution dynamic MRI. Magn Reson Med. 2009;61:103–116. [PubMed]

Feng L, Otazo R, Jung H, Jensen JH, Ye JC, Sodickson DK, Kim D. Accelerated cardiac T2 mapping using breath-hold multi-echo fast spin-echo pulse sequence with compressed sensing and parallel imaging. Magn Reson Med. 2011;65:1661–1669. [PMC free article] [PubMed]

Tsao J, Tarnavski O, Privetera M, Shetty S. k-t denoising—exploiting spatiotemporal correlations for signal-to-noise improvement in dynamic imaging.. Proceedings of the 14th Annual Meeting of ISMRM; Seattle, Washington, USA. 2006. p. 690.

Liang Z. Spatiotemporal imaging with partially separable functions.. Proceedings of IEEE International Symposium on Biomedical Imaging:; From Nano to Macro, Arlington. 2007. pp. 988–991.

Pedersen H, Kozerke S, Ringgaard S, Nehrke K, Kim W. k-t PCA: temporally constrained k-t BLAST reconstruction using principal component analysis. Magn Reson Imaging. 2009;63:706–716. [PubMed]

Ding Y, Chung YC, Jekic M, Simonetti OP. A new approach to auto-calibrated dynamic parallel imaging based on the Karhunen-Loeve transform: KL-TSENSE and KL-TGRAPPA. Magn Reson Imaging. 2011;65:1786–1792.

Kim D, Dyvorne HA, Otazo R, Feng L, Sodickson DK, Lee VS. Accelerated phase-contrast cine MRI using k-t SPARSE-SENSE. Magn Reson Med 2012;67(4):1054-1064

Lustig M, Santos J, Donoho D, Pauly J. k-t SPARSE: high frame rate dynamic MRI exploiting spatio-temporal sparsity.. Proceedings of the 14th Annual Meeting of ISMRM; Seattle, Washington, USA. 2006. p. 2420

Otazo R, Kim D, Axel L, Sodickson D. Combination of compressed sensing and parallel imaging for highly accelerated first-pass cardiac perfusion MRI. Magn Reson Med. 2010;64:767–776.

Lustig M, Donoho D, Pauly JM. Sparse MRI: the application of compressed sensing for rapid MR imaging. Magn Reson Med. 2007;58:1182–1195

W. U. Bajwa, J. D. Haupt, G. M. Raz, S. J. Wright, and R. D. Nowak, "Toeplitz-structured compressed sensing matrices," in Proceedings of the IEEE/SP 14th Workshop on Statistical Signal Processing (SSP '07), pp. 294–298, Madison, Wis, USA, August 2007

Heinrich, M.P., Jenkinson, M., Brady, M., Schnabel, J.A. Globally optimal deformable registration on a minimum spanning tree using dense displacement sampling. in: N. Ayache, H. Delingette, P. Golland, K. Mori (Eds.) MICCAI 2012, Part III. Springer, ; 2012

Malczewski K., Stasinski R., "High resolution MRI image reconstruction from a PROPELLER data set of samples", International Journal of Functional Informatics and Personalised Medicine, Volume 1, Number 3/2008, (2008).

[5]   Olcott, P.D. ; Chinn, G. ; Levin, C.S. "Compressed sensing for the multiplexing of PET detectors", Nuclear Science Symposium and Medical Imaging Conference (NSS/MIC), 2011 IEEE

Glockner, Hu. Parallel MR imaging: a user's guide. Radiographics. 2005 Sep-Oct;25(5):1279-97

J.A. Kennedy, O. Israel, A. Frenkel, R. Bar-Shalom, and H. Azhari. Super-resolution in PET imaging. IEEE transac-tions on medical imaging, 25(2):137{147, 2006.

M. Davenport, "The Fundamentals of Compressive Sensing", IEEE Signal Processing Society Online Tutorial Library, April 12, 2013.

Malczewski, K. and Stasiski, R. Super Resolution for Multimedia, Image, and Video Processing Applications. Studies in Computational Intelligence, Volume 231, 2009.

Olcott, P.D. ; Chinn, G. ; Levin, C.S. "Compressed sensing for the multiplexing of PET detectors", Nuclear Science Symposium and Medical Imaging Conference (NSS/MIC), 2011 IEEE.

J. Dijk, A. W. M. van Eekeren, K. Schutte, D. J. J. de Lange, and L. J. van Vliet, "Super-resolution reconstruction for moving point target detection," Opt. Eng., vol. 47, no. 8, 2008.

T. Q. Pham, L. J. van Vliet, and K. Schutte, "Robust fusion of irregularly sampled data using adaptive normalized convolution," J. Appl. Signal Process., vol. 2006, pp. 1–12, 2006.

S. Farsiu, M. D. Robinson, M. Elad, and P. Milanfar, "Fast and robust multi-frame super resolution," IEEE Trans. Image Process., vol. 13, no. 10, pp. 1327–1344, Oct. 2004.

A. J. Patti, M. I. Sezan, and A. M. Tekalp, "Superresolution video reconstruction with arbitrary sampling lattices and nonzero aperture time," IEEE Trans. Image Process., vol. 6, no. 8, pp. 1064–1076, Aug. 1997.

T. Q. Pham, M. Bezuijen, L. J. van Vliet, K. Schutte, and C. L. L. Hendriks, "Performance of optimal registration estimators," in Proc. Vis. Inf. Process. XIV, 2005, vol. 5817, pp. 133–144.

K. Schutte, D. J. J. de Lange, and S. P. van den Broek, "Signal conditioning algorithms for enhanced tactical sensor imagery," in Proc. SPIE: Infrared Imag. Syst.: Design, Anal., Model. and Testing XIV, 2003, vol. 5076, pp. 92–100.

S. Farsiu, M. D. Robinson, M. Elad, and P. Milanfar, "Fast and robust multi-frame super resolution," IEEE Trans. Image Process., vol. 13, no. 10, pp. 1327–1344, Oct. 2004.

T. Q. Pham, M. Bezuijen, L. J. van Vliet, K. Schutte, and C. L. L. Hendriks, "Performance of optimal registration estimators," in Proc. Vis. Inf. Process. XIV, 2005, vol. 5817, pp. 133–144.

Krzysztof Malczewski received his PhD in Image Processing from Poznan University of Technology in 2006. He is currently an Assistant Professor at the Department of Electronics and Telecommunications, Poznan University of Technology, Poznan, Poland. Since 2002 he has been actively involved as a researcher and teacher in the areas of image processing, algorithms, numerical methods, digital signal processing. Up to now he published nearly 100 scientific papers. His current research interests include image resolution enhancement, medical image processing and digital signal processing.